thymine H3 protons.

Guanine-containing DNA fragments recently have been shown to form unusual structures that seem to utilize guanine tetrads to stabilize unimolecular (*6, 7*), bimolecular (*6, 8*), and tetramolecular (*1, 15*) associations. In this report we have described a new example of a tetramolecular complex, one comprised of strands only 9 bp long and therefore suitable for detailed characterization. Biological processes may take advantage of all of these guanine-tetrad–containing structures. For example, four duplexes may form tetraplexes while initiating alignment during meiosis (*1, 15*). Guanine-rich regions within two chromatids may form hairpins and then dimerize, thereby aligning and pairing the strands for recombination (*8*). Dimerization also may occur at telomeric ends (*6, 8*). The guanine-rich strand of a single duplex may separate from its complementary strand to form its own structure, either within the strand (*7*), possibly as part of H DNA (*19*), or at its end (*6*). Control of these different forms may depend in part on a "sodium-potassium switch" (*15*). Furthermore, these guanine self-paired structures may interact with proteins. For example, the enzyme human DNA(cytosine-5)methyltransferase recently was proposed to act at a possible G4-DNA/B-DNA junction at codon 12 of c-H-*ras* (*20*). In addition, the enzyme called telomere terminal transferase appears specifically to act on specialized telomere structures (*21*). Guanine self-associations also may influence RNA structure since guanine tetrads have been postulated to form between strands of poly rG (*11*). Additional biophysical studies on specially designed and synthesized DNA and RNA fragments should help to elucidate the potential role that these guanine associations play in biological systems.

REFERENCES AND NOTES

1. D. Sen and W. Gilbert, *Nature* **334**, 364 (1988).
2. E. H. Blackburn and J. W. Szostak, *Annu. Rev. Biochem.* **53**, 163 (1984).
3. T. Nikaido, Y. Yamawaki-Kataoka, T. Honjo, *J. Biol. Chem.* **257**, 7322 (1982); A. J. Jeffreys, V. Wilson, S. L. Thein, *Nature* **314**, 67 (1985); D. A. Collier, J. A. Griffin, R. D. Wells, *J. Biol. Chem.* **263**, 7397 (1988); N. D. Hastie and R. C. Allshire, *Trends Genet.* **5**, 326 (1989).
4. J. M. Nickol and G. Felsenfeld, *Cell* **35**, 467 (1983); T. Evans, E. Schon, G. Gora-Maslak, J. Patterson, A. Efstratiadis, *Nucleic Acids Res.* **12**, 8043 (1984); M. W. Kilpatrick, A. Torri, D. S. Kang, J. A. Engler, R. D. Wells, *J. Biol. Chem* **261**, 11350 (1986); C. J. Pears and J. G. Williams, *Nucleic Acids Res.* **16**, 8467 (1988).
5. E. Henderson, C. C. Hardin, S. K. Walk, I. Tinoco, Jr., E. H. Blackburn, *Cell* **51**, 899 (1987); E. R. Henderson and E. H. Blackburn, *Mol. Cell. Biol.* **9**, 345 (1989).
6. J. R. Williamson, M. K. Raghuraman, T. R. Cech, *Cell* **59**, 871 (1989).
7. I. G. Panyutin *et al.*, *Proc. Natl. Acad. Sci U S.A.* **87**, 867 (1990).
8. W. I. Sundquist and A. Klug, *Nature* **342**, 825 (1989).
9. M. Gellert, M. N. Lipsett, D. R. Davies, *Proc. Natl. Acad Sci. U.S.A.* **48**, 2013 (1962); J. F. Chantot, M. Sarocchi, W. Guschlbauer, *Biochimie* **53**, 347 (1971); S. B. Zimmerman, *J. Mol. Biol* **106**, 663 (1976).
10. T. J. Pinnavaia *et al.*, *J Am. Chem Soc.* **100**, 3625 (1978); M. Borzo, C. Detellier, P. Laszlo, A. Paris, *ibid.* **102**, 1124 (1980).
11. S. B. Zimmerman, G. H. Cohen, D. R. Davies, *J. Mol. Biol.* **92**, 181 (1975).
12. S. Arnott, R. Chandrasekaran, C. M. Marttila, *Biochem. J.* **141**, 537 (1974).
13. F. B. Howard and H. T. Miles, *Biochemistry* **21**, 6736 (1982).
14. P. Mariani, C. Mazabard, A. Garbesi, G. P. Spada, *J. Am. Chem. Soc.* **111**, 6369 (1989).
15. D. Sen and W. Gilbert, *Nature* **344**, 410 (1990).
16. B. L. Gaffney and R. A. Jones, *Biochemistry* **28**, 5881 (1989).
17. K. J. Breslauer, in *Thermodynamic Data for Biochemistry and Biotechnology*, H. J. Hinz, Ed. (Springer-Verlag, New York, 1986), pp. 402–427; L. A. Marky and K. J. Breslauer, *Biopolymers* **26**, 1601 (1987).
18. Preliminary ultracentrifugation measurements in 1 M NaCl, conducted in collaboration with E. Braswell, suggest that more than one species may be present under the centrifugation conditions. However, meaningful interpretation of these data demands an understanding of the relative contributions of any competing equilibria, which in turn requires careful modeling and fitting.
19. V. I. Lyamichev *et al.*, *Nature* **339**, 634 (1989).
20. S. S. Smith, D. J. Baker, L. A. Jardines, *Biochem Biophys. Res. Commun.* **160**, 1397 (1989).
21. D. Shippen-Lentz and E. H. Blackburn, *Mol. Cell. Biol* **9**, 2761 (1989); C. W. Greider and E. H. Blackburn, *Cell* **51**, 887 (1987).

22. Supported by grants from the National Institutes of Health GM31483 (R.A.J.), GM23509 (K.J.B.) and an American Cancer Society Faculty Research Award to R.A.J.

30 May 1990; accepted 21 August 1990

Underexpression of β Cell High K_m Glucose Transporters in Noninsulin-Dependent Diabetes

JOHN H. JOHNSON, ATSUSHI OGAWA, LING CHEN, LELIO ORCI, CHRISTOPHER B. NEWGARD, TAUSIF ALAM, ROGER H. UNGER*

The role of defective glucose transport in the pathogenesis of noninsulin-dependent diabetes (NIDDM) was examined in Zucker diabetic fatty rats, a model of NIDDM. As in human NIDDM, insulin secretion was unresponsive to 20 mM glucose. Uptake of 3-*O*-methylglucose by islet cells was less than 19% of controls. The β cell glucose transporter (GLUT-2) immunoreactivity and amount of GLUT-2 messenger RNA were profoundly reduced. Whenever fewer than 60% of β cells were GLUT-2–positive, the response to glucose was absent and hyperglycemia exceeded 11 mM plasma glucose. We conclude that in NIDDM underexpression of GLUT-2 messenger RNA lowers high K_m glucose transport in β cells, and thereby impairs glucose-stimulated insulin secretion and prevents correction of hyperglycemia.

TYPE 2 OR NONINSULIN-DEPENDENT diabetes (NIDDM), the most common hyperglycemic syndrome of man, is ascribed to a declining capacity of pancreatic β cells to compensate for underlying insulin resistance by increased secretion of insulin (*1*). The mechanism of this genetically determined β cell decompensation is obscure; β cells of NIDDM patients appear morphologically normal (*2*). The loss of acute insulin response to glucose in such patients is not accompanied by a parallel impairment in the insulin response to non-glucose secretagogues (*3*). This observation points to a glucose-specific defect in the pathway for insulin secretion. Transmembrane glucose transport is one possible site of such a defect (*4–6*).

Here we report that in a rodent model of NIDDM, hyperglycemia in excess of 11 mM is invariably associated with selective β cell unresponsiveness to glucose, reduced glucose transport in islets, and high K_m (Michaelis constant) underexpression of the high K_m glucose transporter of β cells (GLUT-2). We propose that these abnormalities are causally linked.

We employed as a model of NIDDM a colony of partially inbred Zucker diabetic fatty (ZDF) rats [ZDF/Drt-*fa*(F10)] (*7*). In this colony, all of the males develop obesity, insulin resistance, and overt NIDDM between the seventh and ninth week of life. By 10 weeks of age, their average plasma glucose level exceeds 22 mM. The female littermates also develop obesity and insulin resistance but do not become overtly diabetic, presumably because their β cells maintain sufficient glucose-responsive insulin secretion to compensate for the resistance.

To determine whether, as in human NIDDM, β cells of overtly diabetic ZDF rats are insensitive to glucose, we studied

Center for Diabetes Research, University of Texas, Southwestern Medical Center, 5323 Harry Hines Boulevard, Dallas, TX 75235.

*To whom correspondence should be addressed.

obese male ZDF rats with a morning plasma glucose level in excess of 11.1 mM. Because sex-matched nondiabetic obese ZDF males do not exist, we employed as controls age-matched obese nondiabetic females (*fa/fa*) with a similar degree of insulin resistance but without β cell decompensation. As male controls we used age-matched nondiabetic lean male Zucker heterozygotes (*fa/+*) and normal male Wistar rats. Pancreata were isolated and perfused (*8*) with 20 mM glucose, 10 mM arginine, and a combination thereof (Fig. 1). Glucose-stimulated insulin secretion was observed in every nondiabetic control rat, but not in any diabetic ZDF rat with hyperglycemia of 11 mM plasma glucose or above. In diabetic rats with hyperglycemia below 10 mM plasma glucose, the insulin response to glucose was mildly present but subnormal. Baseline insulin secretion and the insulin response to arginine were greater in both the male diabetic and the female nondiabetic ZDF groups than in the nonobese male control groups.

Unrestricted high K_m glucose transport is regarded as essential for normal β cell responsiveness to glucose (*10, 11*). To determine whether the β cell insensitivity to glucose was the result of impaired high K_m glucose transport, we compared the initial velocity of 15 mM 3-*O*-methylglucose (3-*O*-MG) uptake by the isolated islets (*12*) of severely diabetic male ZDF rats with that of nondiabetic female ZDF rats and the two other control groups (Fig. 2). In the diabetic animals the initial rate was 2.7 mmol min^{-1} $liter^{-1}$ of islet space, as compared to 9.2 mmol min^{-1} $liter^{-1}$ in the nondiabetic fatty females and 11.0 and 13.9 mmol min^{-1} $liter^{-1}$ in the lean male heterozygotes and Wistar controls, respectively. This reduction in the initial rate of high K_m glucose transport in the diabetic islets could account for the inability of β cells to discriminate between a normal and an elevated level of plasma glucose.

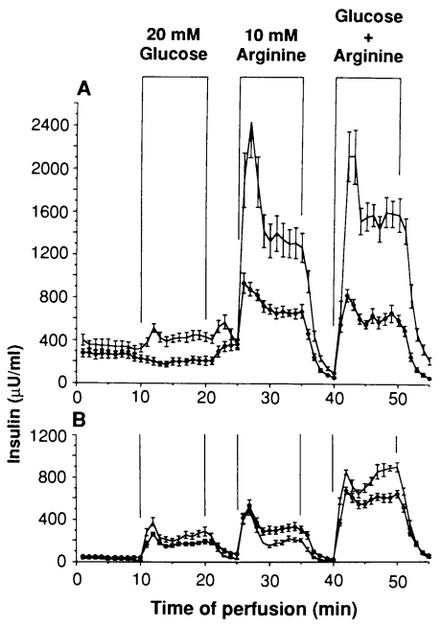

Fig. 1. Insulin response (mean ± SEM) to 20 mM glucose, 10 mM arginine, and combination thereof in isolated perfused pancreata of (**A**) obese male diabetic ZDF rats (n = 8) (●——●) and nondiabetic obese female Zucker rats (n = 9) (——) and (**B**) nondiabetic lean male Zucker rats (n = 9) (●——●) and nondiabetic male Wistar rats (——). The nondiabetic female differed from the nondiabetic lean male in baseline insulin secretion as judged by analysis of variance ($P < 0.001$). The glucose-induced insulin secretion of the diabetic male and the nondiabetic female differed from control groups as judged by analysis of variance ($P < 0.001$).

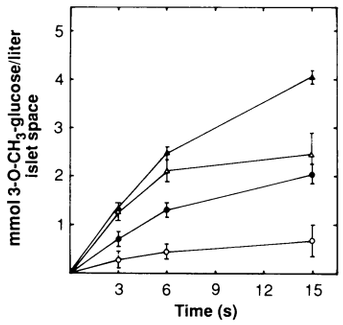

Fig. 2. Time course of uptake of 15 mM 3-*O*-methylglucose by dispersed islet cells pooled from four nondiabetic Wistar rats (▲), four nondiabetic lean male Zucker rats (*fa/+*) (△), eight nondiabetic obese female Zucker rats (*fa/fa*) (●), and eight diabetic obese male Zucker rats (*fa/fa*) (○) (plasma glucose 24.9 to 33.2 mM). All Zucker animals were 12 weeks of age. Each data point represents the mean ± SEM of four independent experiments after correction for nonspecific uptake (L-glucose) in the diabetic and nondiabetic ZDF rats, each of which was carried out in duplicate as described elsewhere (*5, 11*). In the Wistar and lean male Zucker rats two independent experiments were carried out in duplicate.

We next determined whether the reduction in the high K_m 3-*O*-MG uptake was associated with a reduction in the amount of immunodetectable GLUT-2 and its mRNA. The identity in primary sequence between the glucose transporters of rat hepatocytes and β cells (*10, 11*) enabled us to raise an antiserum to a synthetic COOH-terminal hexadecapeptide (*13*) predicted from the sequence of liver GLUT-2 mRNA (*10*). When membrane preparations made from the isolated islets of the three nondiabetic control rats were immunoblotted (*13*) with GLUT-2 antiserum, a prominent 60-kD band was observed (Fig. 3) that was not detected either with preimmune serum or with GLUT-2 antiserum preincubated with the peptide antigen (*13*). This band was not observed in immunoblots of an equivalent amount of islet cell membranes from diabetic ZDF rats with greater than 27.8 mM plasma glucose, and was barely detectable in a fivefold excess of membrane. In ZDF rats with less severe diabetes (11.1 to 16.7 mM plasma glucose) the 60-kD band was present but was reduced in intensity compared to the controls. The band was only slightly reduced (~30%) in hepatocyte membranes from the severely diabetic ZDF rats (*13*). GLUT-2 mRNA in pancreata of severely diabetic ZDF rats was 50 to 63% below controls when quantitated by in situ hybridization (*14*) and 75% below according to densitometric scanning of Northern blots containing polyadenylated [poly(A)$^+$] mRNA isolated from whole pancreata (Table 1). GLUT-2 mRNA was not reduced in the livers of severely diabetic rats. The results indicate that the reduction in the amount of immunodetectable GLUT-2 in β cells is, to a significant degree, associated with a reduction in the amount of GLUT-2 mRNA of β cells.

To determine whether the β cell dysfunction and hyperglycemia of the diabetic ZDF rats were quantitatively related to the loss of GLUT-2, we subjected the pancreata processed after the perfusion experiments (Fig. 1) to immunofluorescence staining for GLUT-2 and insulin (*15*) and determined the percent of GLUT-2–positive β cells (*6*). The functional and metabolic parameters of each rat were then expressed relative to the percent of its β cells displaying immunocytochemically detectable GLUT-2 (Fig. 4). We found a significant negative relation between hyperglycemia and the percent of

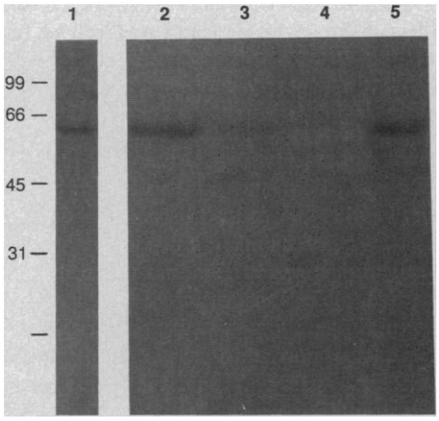

Fig. 3. Immunoblot for GLUT-2 in crude islet membrane preparations (*13*) from nondiabetic Wistar rats (lane 1), nondiabetic lean male Zucker rats (*fa/+*) (lane 2), 8-week-old male Zucker diabetic fatty rats (glucose 13.6 mM) (lane 3), 12-week-old male Zucker diabetic fatty rats (glucose 25.3 mM) (lane 4), and 12-week-old female nondiabetic Zucker fatty rats (lane 5). The band with an apparent M_r of 60 kD is blocked by preincubation of the antibody with a 10^3 M excess of antigen (*13*). The second band with an apparent M_r 50 kD is detected with preimmune serum and is not blocked by antigen excess. It is not detected in islet membranes of Wistar rats.

Table 1. GLUT-2 mRNA in pancreas of diabetic ZDF males and age-matched controls. (**A**) Signal grain density of pancreatic sections hybridized in situ (*14*) expressed as reciprocals of reading exposure time of dark-field images (mean ± SEM) islets in each group of animals. $P < 0.001$ by analysis of variance, 0.05 by Student–Newman-Keuls test, showing that all three groups are significantly different. (**B**) Ratio of GLUT-2/elastase poly(A)$^+$ mRNA isolated from whole pancreata. Calculations are based on densitometric analysis of Northern (RNA) blots. Northern blotting of whole pancreas poly(A)$^+$ RNA was carried out with the same GLUT-2 mRNA probe labeled with ^{32}P. Blots were also hybridized with an elastase antisense mRNA probe as an index of the amount of pancreatic RNA applied to the gel.

	A	B
Diabetic male ZDF rats (*fa/fa*) (plasma glucose >11 mM)	0.09 ± 0.0073 (n = 25)	0.22
Nondiabetic fatty females (*fa/fa*)	0.18 ± 0.0110 (n = 20)	0.9
Nondiabetic lean males (*fa/+*)	0.24 ± 0.0196 (n = 20)	0.74

GLUT-2–positive β cells (for $\log_{10}$ of plasma glucose the slope ± standard error was −0.0084 ± 0.0010; $P < 0.001$) (*16*) (Fig. 4A). In every rat with less than 60% β cells positive for GLUT-2, the morning blood glucose was over 11 mM (200 mg/dl) (Fig. 4A), and glucose-stimulated insulin secretion was absent (Fig. 4B). Basal insulin secretion, which was high in the mildly diabetic rats with β cell GLUT-2 immunofluorescence above 60%, declined in parallel with the fall in GLUT-2 immunofluorescence to quantities below 60% (slope ± standard error was 4.513 ± 1.273; P = 0.012) (Fig. 4C). By contrast, arginine-stimulated insulin secretion was independent of the level of GLUT-2 immunofluorescence (Fig. 4D).

These findings indicate that the hyperglycemia of NIDDM in ZDF rats, as in human NIDDM, is associated with selective loss of glucose-stimulated insulin secretion. The rate of high K_m glucose transport in the islets of severely diabetic rats was reduced to 18% or less of controls, which could well explain the glucose insensitivity of their β cells.

Glucose transport in normal β cells is estimated to have a K_m of ~17 mM (*11*); at this high K_m, glucose transport is never rate-limiting for glucokinase-catalyzed phosphorylation (*9*). An incremental increase in extracellular glucose from a normal fasting level (4 to 5 mM) to a normal postprandial level (8 to 10 mM) will be reflected by a proportionate increase in intracellular glucose, thus causing a glucokinase-mediated increase in glucose usage and an appropriate increase in insulin release. We calculate from rates of transport measured at physiologic blood glucose levels that a 75% reduction in high K_m transport would reduce glucose transport to rates that could limit glucose usage by islets (*9, 11*). In this case a postprandial rise in glucose to above 5 mM would not increase intracellular glucose usage and could not stimulate insulin secretion. Failure to mount an appropriate insulin response to a rise in glucose concentration will result in the hyperglycemia upon which the diagnosis of NIDDM is based.

The issue of primacy of the reduced expression of GLUT-2 in the pathogenesis of the β cell failure has not been addressed here. However, GLUT-2 down-regulation does not appear to be secondary to hyperglycemia (*6*), which increases β cell GLUT-2 mRNA in normal rats (*15*). Conversely, chronic administration of the α-glucosidase inhibitor, acarbose, to prediabetic male ZDF rats prevents their hyperglycemia but does not prevent the GLUT-2 deficiency (*6*). Although chronic hyperinsulinemia suppresses GLUT-2 mRNA in normal islets (*15*), in β cells of the nondiabetic female Zucker rats, which have even greater basal hyperinsulinemia than the diabetic males, GLUT-2 mRNA was not reduced (Table 1). The down-regulation appears to be relatively tissue-specific inasmuch as neither immunodetectable GLUT-2 nor its mRNA were comparably reduced in hepatocytes of the diabetic rats.

Reduction in β cell GLUT-2 appears to be the most proximal abnormality thus far identified in NIDDM. The putative pathogenesis of the β cell disorder now seems to be as follows: an unknown factor leads to reduced GLUT-2 expression and therefore a reduced capacity for high K_m glucose transport, which in turn results in loss of glucose-stimulated insulin response and uncorrected hyperglycemia. If GLUT-2 is also underexpressed in humans with NIDDM, elucidation of the mechanisms of this abnormality could lead to new therapeutic strategies designed to restore the glucose responsiveness of β cells in these patients, and thereby improve their capacity to compensate for the underlying insulin resistance.

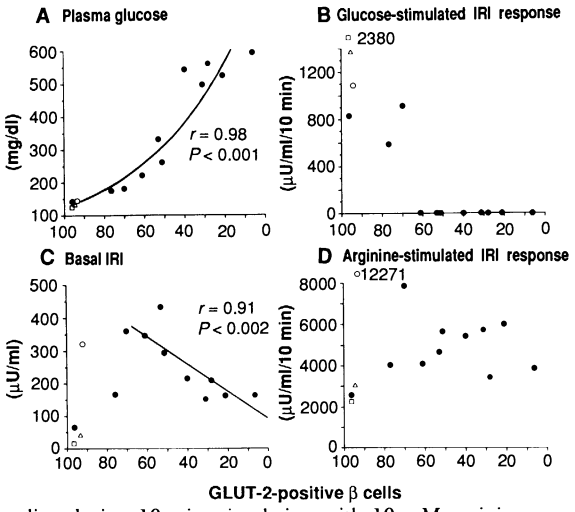

Fig. 4. Relationships between islet cell function and immunostainable GLUT-2 β cells in pancreata of obese male diabetic ZDF (*fa/fa*) rats (●), nondiabetic obese female (*fa/fa*) (○), nondiabetic lean male (*fa/+*) (△), and nondiabetic Wistar male rats (□). (**A**) Plasma glucose concentration immediately before isolation of the pancreas as a function of percentage of GLUT-2–positive β cells (*16*). (**B**) The increase of IRI (immunoreactive insulin) above baseline IRI during 10-min stimulation of islet pancreas with 20 mM glucose as a function of percentage of GLUT-2–positive β cells. (**C**) Basal or prestimulatory IRI (average of last three values before stimulation) as a function of percentage of GLUT-2–positive β cells. (**D**) The increase in IRI above baseline during 10-min stimulation with 10 mM arginine as a function of percentage of GLUT-2–positive β cells.

REFERENCES AND NOTES

1. R. A. DeFronzo and E. Ferranini, *Medicine* **61**, 125 (1982); G. C. Weir, *Am. J. Med* **73**, 461 (1982); R. A. DeFronzo, *Diabetes* **37**, 667 (1988); G. M. Reaven, *ibid.*, p. 1595 (1988); S. Lillioja, *N Engl J. Med.* **318**, 1217 (1988).
2. Y. Stefan *et al.*, *Diabetes* **31**, 694 (1982); J. Rahier, R. M. Goebbels, J. C. Henquin, *Diabetologia* **24**, 366 (1983).
3. E. Cerasi, R. Luft, S. Efendic, *Diabetes* **21**, 224 (1971); J. P. Palmer, J. W. Benson, R. M. Walter, J. W. Ensinck, *J. Clin Invest* **58**, 565 (1976); M. A. Pfeiffer, J. B. Halter, D. Porte, Jr., *Am J Med* **70**, 579 (1980).
4. R. H. Unger and S. Grundy, *Diabetologia* **28**, 119 (1985); A. Starke, S. Grundy, J. D. McGarry, R. H. Unger, *Proc. Natl Acad. Sci. U.S.A.* **82**, 1544 (1985).
5. J. H. Johnson, B. P. Crider, S. K. McCorkle, M. Alford, R. H. Unger, *N Engl J Med* **322**, 653 (1990).
6. L. Orci *et al.*, unpublished observations.
7. J. B. Clark, C. J. Palmer, W. N. Shaw, *Proc. Soc. Exp. Biol Med* **173**, 68 (1983).
8. G. M. Grodsky and R. E. Fanska, *Methods Enzymol.* **39**, 364 (1975); M. Tominaga, *Proc Natl. Acad. Sci U.S.A.* **83**, 9749 (1986).
9. M. D. Meglasson and F. M. Matschinsky, *Diabetes Metab. Rev.* **2**, 153 (1986).
10. B. Thorens, H. K. Sarkar, H. R. Kaback, H. F. Lodish, *Cell* **55**, 281 (1988).
11. J. H. Johnson, C. B. Newgard, J. L. Milburn, H. F. Lodish, B. Thorens, *J. Biol. Chem* **265**, 6548 (1990).
12. Islet isolation [S. P. Naber *et al*, *Diabetologia* **19**, 439 (1980)] and EGTA dispersal of islet cells was per-

formed as previously described (*5*), except that pancreata from obese Zucker females and Zucker diabetic fatty males were subjected to a second 16-min collagenase digestion using half strength (0.25%) collagenase before Ficoll purification of islets. This was necessary because of the increase in fibrous tissue in both groups. The uptake of 3-*O*-methyl-β-D-glucose and L-glucose was measured as previously described (*5*).

13. Anti-GLUT-2 antibody #1092 was raised against COOH-terminal hexadecapeptide RKATVQME-FLGSSETV predicted from the DNA sequence of GLUT-2 (*10*) and synthesized by S. Stradley and L. Gierasch, University of Texas Southwestern Medical Center. The peptide was coupled to purified protein derivative (PPD) by the method of Lachmann *et al.* [P. J. Lachmann, L. Strangeways, A. Vyakarnam, G. Evan, in *Synthetic Peptides as Antigens*, R. Porter and J. Whelan, Eds. (Ciba Foundation Symposium, 1986), vol. 119, pp. 25–57] and was injected with Freund's complete adjuvant subcutaneously into New Zealand white rabbits. Rabbits were boosted after 6 weeks with PPD-coupled peptide suspended in Fruend's incomplete adjuvant. Crude islet membrane preparations were made by homogenizing whole islets suspended in 50 mM Hepes, pH 7.4, 250 mM sucrose, 1 mM EDTA, and 1 mM trasylol with 20 strokes of a Teflon-glass Potter-Elvehjem homogenizer (*14*). After centrifugation at 25,000*g* for 20 min at 4°C, the sediment was resuspended in homogenizing buffer, layered over 40% sucrose, and centrifuged at 150,000*g* for 2 hours at 4°C in an SW 41 rotor. After harvesting the crude membranes from the 40% sucrose–overlay interface the membranes were resedimented and solubilized in the appropriate amount of digestion buffer for SDS–polyacrylamide gel electrophoresis [U. K. Laemmli, *Nature* **227**, 680 (1970)]. Following electrophoresis and electrotransfer to nitrocellulose filters (Bio-Rad), the filters were blocked with 10 mM tris, pH 7.4, 0.15 mM NaCl, 10 mM EGTA, 0.1% Tween 20, and 5% bovine serum albumin (BSA). The filters were incubated at room temperature for 2 hours in the above buffer containing 0.5% BSA and a 5×10^4 dilution of rabbit antibody against rat GLUT-2, washed and developed with 10^6 cpm/ml ^{125}I goat Fab antibody to rabbit immunoglobulin G.
14. L. Chen *et al.*, *Proc. Natl. Acad Sci. U.S.A.* **87**, 4088 (1990). All pancreata were perfused with 4% paraformaldehyde and 0.05% glutaraldehyde. Frozen tissue sections were hybridized [D. M. Simmons, J. L. Arizza, L. W. Swanson, *J. Histotechnol.* **12**, 169 (1986)] with 5×10^6 dpm/ml of ^{35}S-labeled antisense GLUT-2 RNA in 50% formamide at 55°C overnight. After ribonuclease treatment and washing under stringent conditions, the slides were dipped in Kodak NTB-3 emulsion and exposed in the dark for 1 week. Density of GLUT-2 mRNA hybridization was measured with the use of the spot meter of a Nikon microscope photographic VFXIIA system at constant light setting and ASA 100. Reciprocals of reading exposure time of individual islets in dark-field image were used to represent the signal grain density after correcting for the background. Twenty randomly picked islets from each group of rats were measured.
15. L. Orci, B. Thorens, M. Ravazzola, H. F. Lodish, *Science* **245**, 295 (1989).
16. The curve in Fig. 4A was linearized to obtain the slope. The equation of the curve is $y = 824.1 \times 10^{-0.0084x}$, where y is plasma glucose and x is percentage of GLUT-2–positive β cells. In linearized form, this is $\log_{10} y = 2.916 - 0.0084x$.
17. We thank M. S. Brown, D. W. Foster, and K. L. Luskey, for reading this manuscript, R. Risser, for statistical analyses, T. Autrey for excellent secretarial work and K. McCorkle for expert technical assistance. Supported by NIH grant DK02700-30, Veterans Administration Institutional Research Support grant 549-8000, Research and Education Foundation, Juvenile Diabetes Foundation grant 187417, Swiss National Science Foundation grant 31-26625,89, American Diabetes Association Research and Education Foundation, American Heart Association–Texas affiliate.

8 May 1990; accepted 14 August 1990

Involvement of the Silencer and UAS Binding Protein RAP1 in Regulation of Telomere Length

ARTHUR J. LUSTIG,* STEPHEN KURTZ, DAVID SHORE

The yeast protein RAP1, initially described as a transcriptional regulator, binds in vitro to sequences found in a number of seemingly unrelated genomic loci. These include the silencers at the transcriptionally repressed mating-type genes, the promoters of many genes important for cell growth, and the poly[(cytosine)$_{1-3}$ adenine] [poly($C_{1-3}A$)] repeats of telomeres. Because RAP1 binds in vitro to the poly($C_{1-3}A$) repeats of telomeres, it has been suggested that RAP1 may be involved in telomere function in vivo. In order to test this hypothesis, the telomere tract lengths of yeast strains that contained conditionally lethal (ts) *rap1* mutations were analyzed. Several *rap1^{ts}* alleles reduced telomere length in a temperature-dependent manner. In addition, plasmids that contain small, synthetic telomeres with intact or mutant RAP1 binding sites were tested for their ability to function as substrates for poly($C_{1-3}A$) addition in vivo. Mutations in the RAP1 binding sites reduced the efficiency of the addition reaction.

THE TELOMERES OF ALL EUKARYOTES examined thus far consist of a guanine-cytosine (GC)–rich sequence of variable length [for example, poly($C_{1-3}A$) in *Saccharomyces cerevisiae*] (*1*). The G-rich strand appears to be added in a DNA template–independent process that requires telomerase, a ribonucleoprotein (*2*). In several organisms, the sequences present at telomeres are organized into an altered chromatin structure that is resistant to degradation by micrococcal nuclease (*3, 4*). In yeast and ciliates, nonhistone proteins that bind telomere sequences have been identified (*4, 5*). The interaction of these proteins with telomeric DNA is likely to be important for the control of telomere replication, association, and higher order structure (*1*).

In *S. cerevisiae*, the predominant telomere-binding protein is RAP1 (also known as TBA, GRF1, and TUF1) (*5–7*). Telomeric binding sites for RAP1 [ACACCCA-CACACC] are found at an average density of one site per 40 bp of telomeric poly($C_{1-3}A$) (*8, 9*). The gene encoding RAP1 has been cloned and is essential for viability (*7*).

To investigate whether RAP1 affects telomere structure in vivo, we analyzed chromosomal telomere lengths in four independent *rap1^{ts}* mutants. Each mutant allele was a unique recessive missense mutation and displayed a distinct pattern of growth. Strains that contained the *rap1-2* or *rap1-5* alleles grew at or near wild-type rates under permissive conditions (23°C) and required at least 16 hours of incubation at the restrictive temperature (37°C) to inhibit growth. Strains that carried either the *rap1-1* or *rap1-4* alleles grew poorly at 23°C and rapidly arrested growth when shifted to 37°C.

The effect of the *rap1^{ts}* mutations on the size of telomeric poly($C_{1-3}A$) tracts was analyzed by culturing each mutant strain at permissive or semipermissive temperatures for approximately 100 generations. The semipermissive temperature was defined as the temperature at which a significant decrease in growth rate occurred. Under these conditions, cells were partially deficient in RAP1 activity. The tract length of the predominant class of telomeres (the XY′ class, see Fig. 1A) was measured by hybridizing Southern (DNA) blots of Xho I–digested genomic DNA with ^{32}P-labeled poly[d(GT)]·poly-[d(CA)], which identified the telomeric poly($C_{1-3}A$) sequences and internal poly(CA) tracts (Fig. 1A).

At the permissive temperature (23°C), telomeres showed only minimal alterations in tract length (Fig. 1B). However, at semipermissive temperatures (30° to 31.5°C), telomere tract size was gradually reduced in *rap1^{ts}* cells during ~100 generations of culturing (300 to 125 bp, Fig. 1C). Progressive loss of sequences, observed in both *rap1-2* mutant haploids and homozygous diploids, was recessive; diploids that were heterozygous for the *rap1-2* mutation had wild-type tract lengths (*10*). Strains containing either the *rap1-4* or the *rap1-1* allele showed a moderate loss of telomeric sequences (~130 and ~88 bp, respectively) when cultured at 23°C (*10*). No significant changes in telomere sizes were observed in isogenic wild-type strains at any of the temperatures used in this study (Fig. 1, B and C).

The loss of terminal tracts observed in *rap1-2* mutants was fully reversible. When

A. J. Lustig, Department of Molecular Biology, Memorial Sloan-Kettering Cancer Center, New York, NY 10021.
S. Kurtz and D. Shore, Department of Microbiology, College of Physicians and Surgeons, Columbia University, New York, NY 10032.

*To whom correspondence should be addressed.